

See discussions, stats, and author profiles for this publication at: <https://www.researchgate.net/publication/8341585>

# Revealing the Configuration and Crystal Packing of Organic Compounds by Solid-State NMR Spectroscopy: Methoxycarbonylurea, a Case Study

ARTICLE *in* CHEMISTRY · OCTOBER 2004

Impact Factor: 5.73 · DOI: 10.1002/chem.200400191 · Source: PubMed

---

CITATIONS

13

---

READS

22

3 AUTHORS, INCLUDING:



[Sven Macholl](#)

Barts Cancer Institute

27 PUBLICATIONS 378 CITATIONS

[SEE PROFILE](#)



[Gerd Buntkowsky](#)

Technical University Darmstadt

225 PUBLICATIONS 3,206 CITATIONS

[SEE PROFILE](#)

# Revealing the Configuration and Crystal Packing of Organic Compounds by Solid-State NMR Spectroscopy: Methoxycarbonylurea, a Case Study

Sven Macholl,<sup>[a, b]</sup> Frank Börner,<sup>[c]</sup> and Gerd Buntkowsky<sup>\*[a]</sup>

**Abstract:** The molecular configuration and intermolecular arrangement of polycrystalline methoxycarbonylurea (MCU) has been studied by a combination of chemical editing, rotational echo double resonance (REDOR) spectroscopy and ab initio calculations. From the multispin  $IS_n$  REDOR experiments several dipolar couplings were determined and converted into distance constraints. Intra- and intermolecular dipolar couplings were distinguished by isotope dilution. The configuration of the MCU molecule can be determined from three torsion

angles  $\Psi_1$ ,  $\Psi_2$ , and  $\Psi_3$ . Ab initio calculations showed that these angles are either  $0^\circ$  or  $180^\circ$  (*Z* or *E*). From the REDOR experiments, the *E* configuration was found for  $\Psi_1$  and  $\Psi_2$  and the *Z* configuration for  $\Psi_3$ . Thus the configuration of MCU in the solid state was determined to be *EEZ*. Distance constraints for the intermolecular ar-

**Keywords:** configuration determination • hydrogen bonds • molecular packing • NMR crystallography • REDOR

rangement of MCU were obtained by performing REDOR experiments on  $^{13}C^{15}N_2$  MCU with different degrees of isotope dilution and on a cocrystallized 1:1 mixture of  $^{13}C$ (urea) MCU and  $^{15}N$ (amide) MCU. By combining these distance constraints with molecular modeling, three different possible packing motifs for MCU molecules were found. The molecules in these motifs are arranged as linear chains with methoxy groups at the borders of the chains. All the intermolecular hydrogen bond donors and acceptors in the interior of the chain are saturated.

## Introduction

In a recent study supported by BASF AG,<sup>[1]</sup> methoxycarbonylurea (MCU) and other related urea compounds were investigated as potential long-term nitrogen fertilizers with intermediate solubility in water. Understanding the solubility properties of MCU could help in the more efficient screening of the fertilizer properties of other urea derivatives. For this, detailed knowledge of the molecular configuration and intra- and intermolecular hydrogen-bonding properties of the urea compounds is necessary. Single-crystal X-ray crystallography could not be applied to the system because the

single crystals exhibit lattice disorder. Recently we reported a static dipolar solid-state NMR study of MCU<sup>[2]</sup>.

For the study reported herein, we chose a more general strategy. The molecular configuration of MCU in the solid state was studied by a combination of selective  $^{13}C$  and/or  $^{15}N$ -isotope labeling schemes (chemical editing), dipolar solid-state NMR spectroscopy<sup>[3]</sup> and ab initio calculations. The experimental NMR data were used to obtain a network of interatomic distance constraints. These constraints were converted into torsion angles, which yielded the molecular configuration. Additionally, intermolecular distances provide hints about the intermolecular arrangement of MCU in the crystal (NMR crystallography).<sup>[4–7]</sup>

Our strategy was based on the following basic idea: that the nitrogen and all the carbon atoms, except for the methoxy group, of the amide, urea and ester functions of the MCU molecule (see Figures 1–3) are expected to be mainly  $sp^2$  hybridized. In this case, the C–N bonds show some double-bond character and a planar arrangement is formed (apart from the H(methoxy) atoms). This assumption is supported by results of our previous study<sup>[2]</sup> and by ab initio calculations reported in this study (see below). By using bond lengths and bond angles derived from a geometry optimization by a molecular modeling program, the secondary structure of the MCU backbone is characterized by three torsion angles  $\Psi_1$ ,  $\Psi_2$  and  $\Psi_3$  (see Figure 2). Owing to the

[a] Dr. S. Macholl, Dr. G. Buntkowsky  
Institut für Chemie, Freie Universität Berlin  
Takustrasse 3, 14195 Berlin (Germany)  
Fax: (+49) 30-838-55310  
E-mail: bunt@chemie.fu-berlin.de

[b] Dr. S. Macholl  
Present address: Institut für Biometrie und Medizinische Informatik  
Abteilung Experimentelle Bildverarbeitung  
Otto-von-Guericke-Universität Magdeburg  
Leipziger Strasse 44, 39120 Magdeburg (Germany)

[c] Dr. F. Börner  
Fraunhofer-Institut für Angewandte Polymerforschung  
Postfach 126, 14476 Golm (Germany)

$sp^2$  hybridization and the absence of steric effects, they are expected to be either  $0^\circ$  or  $180^\circ$ .

There are two different solid-state NMR (SSNMR) strategies for determining the torsion angles, namely 1) the correlation of different chemical shift tensors<sup>[8]</sup> and 2) the NMR measurement of intramolecular distances, which constrain the torsion angles.<sup>[9–15]</sup> In this study, the second strategy was employed and heteronuclear dipolar couplings between  $^{13}\text{C}$  and  $^{15}\text{N}$  spins were measured by REDOR NMR.<sup>[16]</sup> These dipolar couplings (the specification “heteronuclear” is omitted from now on) were converted to internuclear distances and the torsion angles adjusted to match these distances.

The optimal selection of isotopomers for the structure determination was crucial to this study. The following points had to be considered: 1) the labeling scheme should give an unambiguous structure; 2) the number of necessary isotopomers should be minimized; 3) the chemical synthesis should be easy and cost efficient; 4) the measured dipolar interactions should be in a range in which the REDOR experiments exhibit high sensitivity and yield accurate distances.

To fulfil all these conditions, we started with a numerical simulation of the possible molecular structures and the corresponding dipolar interactions. The structural calculations were performed by employing the molecular modeling program SPARTAN.<sup>[17]</sup> The calculations show that there are six sterically allowed configurations of MCU, namely three configurations without and three configurations with an intramolecular hydrogen bonds (see first and second column in Figure 1).

In the REDOR experiments, internuclear distances were determined between selectively spin-labeled (in this study  $^{13}\text{C}$  and  $^{15}\text{N}$ ) positions. Figure 1 shows that, in principle, the correct configuration of a planar molecule could be determined from a single  $^{15}\text{N}(\text{amide})$ – $^{13}\text{C}(\text{methoxy})$  distance measurement. In practice, however, it is very difficult to accurately measure C–N distances larger than about 5 Å with

REDOR because of the  $T_2$  relaxation of the observed nucleus. This fact renders most of the possible configurations for MCU indistinguishable by this method. Therefore, it is advantageous to measure shorter distances, preferably between atoms that are separated by three bonds, and thus define a single torsion angle. The full configuration of the molecule can be obtained by the determination of a sufficiently large set of torsion angles by employing a suitable set of isotopomers. For MCU, three doubly spin-labeled molecules may be chosen for this purpose (see Figure 2b–d).

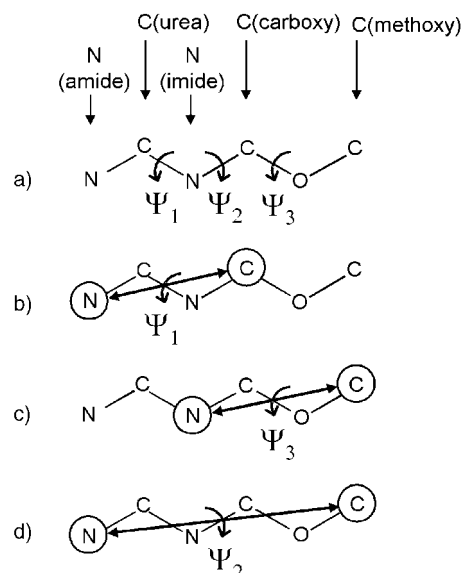


Figure 2. The molecular backbone of MCU with the three torsion angles  $\Psi_n$  ( $n=1,2,3$ ) indicated. Sketches b) to d) illustrate, which C–N distances are used to determine which torsion angle.

With the isotopomers depicted in Figure 2b and 2c, the  $^{15}\text{N}(\text{amide})$ – $^{13}\text{C}(\text{carbamate})$  and  $^{15}\text{N}(\text{imide})$ – $^{13}\text{C}(\text{methoxy})$  distances can be obtained, which yield the torsion angles  $\Psi_1$  and  $\Psi_3$ . Having fixed the terminal parts of the backbone of MCU, the torsion angle  $\Psi_2$  can be determined from a third doubly spin-labeled molecule by using the  $^{15}\text{N}(\text{amide})$ – $^{13}\text{C}(\text{methoxy})$  distance (see Figure 2d), which determines the configuration of the molecule uniquely.

The number of spin-labeled samples necessary to determine the configuration can be reduced by the simultaneous measurement of several dipolar couplings by employing either 1)  $^{13}\text{C}$  (natural abundance), singly  $^{15}\text{N}$ -labeled REDOR spectroscopy<sup>[9]</sup> or 2) REDOR on multispin labeled samples (e.g.,  $^{13}\text{C}^{15}\text{N}_2$ ). The

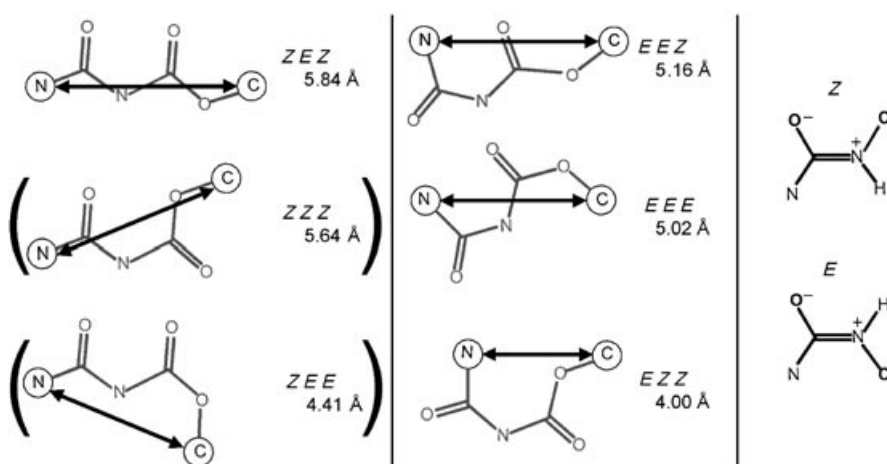


Figure 1. Sketches of the six sterically allowed configurations of MCU; hydrogen atoms are omitted for clarity. Configurations with and without intramolecular hydrogen bonds are in the middle and left panels, respectively. The configurations are denoted using *E,Z* nomenclature (see right panel for an example). The numbers are the calculated distances between the terminal N(amide) and C(methoxy) atoms (encircled). The configurations in parentheses are excluded as possible structures by ab initio calculations.

second method has the advantage of better signal-to-noise, but the more complex spin system necessitates a more elaborate evaluation of the resulting REDOR data. If the individual couplings are sufficiently strong this evaluation can be solved by the so-called REDOR transform.<sup>[18,19]</sup> Alternatively a full simulation of the experimental spin system can be performed<sup>[20–22]</sup> or specialized REDOR sequences like REDOR 3D,<sup>[23]</sup> FDR-REDOR,<sup>[24,25]</sup>  $\theta$ -REDOR,<sup>[26]</sup> or MS REDOR<sup>[27]</sup> can be employed, which however cause substantially longer measuring times.

In this contribution both kinds of experiments, namely 1)  $^{13}\text{C}$  (natural abundance), singly  $^{15}\text{N}$ -labeled REDOR spectroscopy and 2) REDOR on  $\text{IS}_n$  spin systems, were combined. The experimental REDOR data of the  $\text{IS}_n$  spin systems were evaluated by full numerical simulations of the spin system.

In pure solid phases of relatively small molecules like MCU, the intramolecular and intermolecular distances between spin labels may be the same. To distinguish between these cases isotope dilution in unlabeled material is generally necessary.

The rest of the article is organized as follows. First a brief survey of the sample preparation and characterization is given, followed by our experimental setup and a description of the experiments and calculations. Next, the experimental results are presented, discussed and finally summarized.

## Experimental Section

The considerations discussed in the introduction show that it should be possible to obtain the three torsion angles from only two suitable spin-labeled samples. The labeled isotopomers and the observable intramolecular dipolar couplings are shown in Figure 3. For the first isotopomer we chose singly  $^{15}\text{N}$ (amide)-labeled MCU for  $^{13}\text{C}$  (natural abundance)  $^{15}\text{N}$  REDOR experiments (the observed nucleus is named first and is underlined). In principle, three intramolecular C–N distances can be determined simultaneously (see Figure 3a) from this sample, which are used

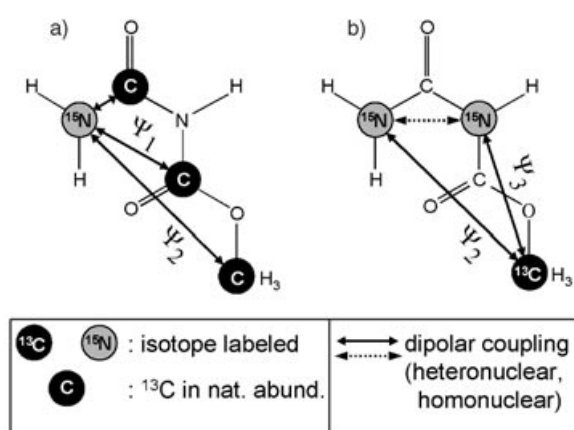


Figure 3. The labeling strategy used in this study for the determination of the torsion angles: a)  $^{15}\text{N}$ (amide)-labeled MCU is studied in a  $^{13}\text{C}$ (natural abundance)  $^{15}\text{N}$  REDOR experiment to determine  $\Psi_1$  and  $\Psi_2$ , b) both  $^{15}\text{N}$  and  $^{13}\text{C}$ (methoxy) atoms are labeled for the determination of  $\Psi_2$  and  $\Psi_3$ . Heteronuclear dipolar couplings are indicated by solid double arrows and the  $^{15}\text{N}$  homonuclear dipolar coupling is indicated by a dotted double arrow.

for the determination of the torsion angles  $\Psi_1$  and  $\Psi_2$ . To determine  $\Psi_3$ , a satisfactory signal-to-noise level requires a longer measuring time. Therefore, we chose a more favorable experiment to determine  $\Psi_3$ , which, however, required the synthesis of a  $^{15}\text{N}$ (imide)-labeled sample. While the synthesis of the  $^{15}\text{N}$ (amide)-labeled MCU can be accomplished by standard procedures, the synthesis of selectively  $^{15}\text{N}$ (imide)-labeled MCU is rather complicated and expensive. Therefore, as an alternative to the  $^{15}\text{N}$ (imide) sample, we chose to use doubly  $^{15}\text{N}$ -labeled MCU as the second isotopomer by employing commercially available  $^{15}\text{N}_2$ -labeled urea as the starting reagent. Since the quantitative evaluation of two simultaneous  $^{13}\text{C}$ – $^{15}\text{N}$  dipolar couplings in a  $^{13}\text{C}$ – $^{15}\text{N}$  experiment is rather elaborate, we studied this sample in a  $^{15}\text{N}$ – $^{13}\text{C}$  REDOR experiment first. For this experiment we introduced a  $^{13}\text{C}$  label at the methoxy position as dephasing spin:  $^{13}\text{C}$ (methoxy)- $^{15}\text{N}_2$  MCU ( $^{13}\text{C}$ – $^{15}\text{N}_2$  MCU for short). This labeling pattern allows the simultaneous measurement of two  $^{13}\text{C}$ – $^{15}\text{N}$  dipolar couplings (see Figure 3b) in the  $^{15}\text{N}$ – $^{13}\text{C}$  REDOR experiment. These dipolar couplings are used to determine the torsion angles  $\Psi_2$  and  $\Psi_3$ . Note that the influence of the homonuclear  $^{15}\text{N}$ – $^{15}\text{N}$  dipolar interaction on the REDOR signal can be neglected, as explained below in detail.

**Sample preparation and characterization:** All unlabeled and labeled samples used in this study were synthesized in house. The chemical synthesis of the samples is given elsewhere.<sup>[2]</sup> Enrichment in  $^{13}\text{C}$  and  $^{15}\text{N}$  is between 97 and 99%. Triuret, which was obtained as a side product, was removed by recrystallization from water. The absence of solvent molecules in the microcrystalline material was checked by elementary analysis (water) and  $^{13}\text{C}$  SSNMR spectroscopy (organic solvents).  $^1\text{H}$  and  $^{13}\text{C}$  NMR spectra of labeled MCU in  $[\text{D}_6]\text{DMSO}$  samples revealed chemical shifts and several  $J$  couplings, and these have been presented and discussed in reference [2].

**Ab initio calculations:** All quantum-chemical calculations of geometry, energy and vibrations were carried out with the GAUSSIAN98 program<sup>[28]</sup> on an Origin 2000 (SGI) computer with 16 processors MIPS R10000 and 3 GB of memory. The ab initio methods used were Hartree–Fock (HF) and density functional theory (DFT) with the B3LYP functional,<sup>[29,30]</sup> combined with the 3-21G or 6-31G standard basis set for the initial geometry optimizations and then with 6-31++G(d,p) to model the hydrogen bonds. All the data reported here are from B3LYP calculations. After each geometry optimization, the vibrational frequencies were calculated to ensure that the obtained geometry corresponds to a (local) minimum on the potential hypersurface.

**Solid-state NMR spectroscopy:** All SSNMR measurements were performed at room temperature on a commercial Varian InfinityPlus 600 NMR spectrometer operating at a field of 14 T. The resonance frequencies were 599.97 MHz for  $^1\text{H}$ , 150.87 MHz for  $^{13}\text{C}$  and 60.79 MHz for  $^{15}\text{N}$ . For all the experiments, a triply tuned Chemagnetics 5 mm MAS probe of T3 type was used. The powdered samples were packed into zirconium oxide rotors. The spinning frequency of the sample was adjusted in the range of 1 to 10 kHz and was stabilized to approximately  $\pm 2$  Hz. Typical  $\pi$  pulse lengths were 9.7  $\mu\text{s}$  for the  $^{13}\text{C}$  channel and 19.6  $\mu\text{s}$  for the  $^{15}\text{N}$  channel. For 1D spectra, the CPMAS technique was combined with a rotor synchronized Hahn echo, which eliminates the dead time of the probe. Residual  $^1\text{H}$ X dipolar couplings were suppressed using TPPM decoupling<sup>[31]</sup> with a  $B_1$  field of 50 kHz. Ramped amplitude cross-polarization (RAMP-CP)<sup>[32]</sup> was used to enhance the CP efficacy at high spinning rates. Referencing of the CP-MAS spectra to TMS ( $^{13}\text{C}$ ) and  $\text{NH}_3$  was performed by employing adamantane and  $^{15}\text{NH}_4\text{Cl}$ , respectively, as external standards.

All the REDOR spectra were recorded after applying all the recoupling pulses in the non-observed (dephasing) channel. The recoupling pulses were phase-cycled according to the  $xy$ -4 or  $xy$ -8 phase scheme.<sup>[33–35]</sup> Owing to the long spin–lattice relaxation times of MCU (10.4 s at 14 T for  $^1\text{H}$ ) the measurement of a typical REDOR decay curve took approximately 1 day.

**The REDOR experiment:** The basic theory of the REDOR experiment for two-spin<sup>[16,36–39]</sup> and three-spin systems<sup>[20,21,40,41]</sup> has been widely reported in the literature and is not reproduced here.

**Data evaluation of the REDOR experiments:** As explained in the results section below, the REDOR decay curves are caused by spin systems of the  $\text{IS}_2$  and  $\text{IS}_3$  type, which include homonuclear couplings between the dephasing S spins. To evaluate these curves, numerical simulations with

laboratory written MATLAB routines and the SIMPSON program package,<sup>[42]</sup> employing the direct method in conjunction with the REPULSION set of 100 angles,<sup>[43]</sup> were performed. The geometry of an IS<sub>2</sub> spin system is defined by two dipolar couplings  $D_1$  and  $D_2$  (or distances  $r_1$  and  $r_2$ ) and the angle  $\theta$  between the dipolar tensors. Because of the symmetry of dipolar tensors, it is sufficient to consider values of  $\theta$  in the interval  $0-\pi/2$ . For each additional dipolar coupling, another dipolar coupling and two angles have to be defined. In practice, IS<sub>2</sub> spin system simulations have been performed by stepping consecutively through  $D_1$ ,  $D_2$ , and  $\theta$ .

To simulate the REDOR curves, all corrections for the enrichment of isotopes and for natural abundance spins, for example, the dephasing effect of a directly bound natural abundance spin S<sub>2</sub> on the observed I spin in the measurement of a long-range dipolar coupling IS<sub>1</sub>, are taken into account. In general, these corrections are of the order of a few percentages in “completely” <sup>13</sup>C/<sup>15</sup>N-labeled materials. The corrections are important in this study especially for the isotope dilution experiment.

Owing to the very rigid nature of the MCU molecule, due to the high bond order of the C–N bonds and the stabilizing effect of the hydrogen-bonding network, no motional correction of the REDOR data for fast vibrational motions<sup>[38]</sup> is necessary.

## Results and Discussion

In this section, the results of our study are presented. First, the outcome of the ab initio calculations is discussed. From these calculations, possible configurations of isolated MCU molecules were determined, which were then probed in the second step by <sup>13</sup>C/<sup>15</sup>N REDOR spectroscopy to determine the actual secondary structure of MCU in the crystal.

**Ab initio calculations:** By employing the six sterically allowed configurations shown in Figure 1 as the starting point, ab initio geometry optimizations were performed. No minima on the energy hypersurface were found for the ZZZ configuration (large negative vibrational frequency) or for the ZEE configuration (see Figure 1, structures in parentheses). The calculation with the ZEE configuration as input showed that if all three torsion angles are free to change the ZEE converges to the ZEZ configuration. If the torsion angle  $\Psi_3$  is kept constant, two negative vibrational frequencies were calculated, which indicates that the calculated structure does not correspond to a (local) minimum of the energy hypersurface. Therefore, the ZZZ and ZEE configurations were excluded and only four configurations from the calculations remained (see Figure 1, structures without parentheses). The relative energies of these four configurations were calculated to be  $EEZ=0$ ,  $EZZ=4.3$ ,  $EEE=10.1$ ,  $ZEZ=10.2$  kcal mol<sup>-1</sup> (torsion angles that are different to those of the global minimum structure  $EEZ$  are in **bold** type).

The calculations reveal structures with the following properties. 1) The most stable gas-phase structure of MCU predicted by the calculations (configuration  $EEZ$ ) coincides with the configuration of the MCU part of methoxycarbonylbiuret-H<sub>2</sub>O (MCB-H<sub>2</sub>O).<sup>[1]</sup> This structure was obtained by X-ray diffraction and it is characterized by an intramolecular, nonlinear hydrogen bond between N(amide) and O(carbamate/carbonyl) with a N–O distance of 2.75 Å. 2) In the structure with the second lowest energy (configuration  $EZZ$ ), the hydrogen bond acceptor is O(methoxy) instead

of O(carbamate/carbonyl) and the heavy atom distance of this hydrogen bond is 2.72 Å. 3) Rotation of the methoxy group by 180° with respect to the global minimum structure  $EEZ$  yields a structure in which the two H(imide) atoms and two out of the three H(methoxy) atoms are closer (configuration  $EEE$ ). However, the internuclear H,H distances are still rather large (ca. 2.2 Å) compared with the sum of two <sup>1</sup>H van der Waals radii. 4) Rotation around  $\Psi_1$  yields the  $ZEZ$  configuration, which is the only configuration without an intramolecular hydrogen bond that could be realized by ab initio calculations.

**<sup>13</sup>C and <sup>15</sup>N CPMAS spectra:** Next, the <sup>13</sup>C (natural abundance) and <sup>15</sup>N CPMAS spectra of unlabeled and <sup>13</sup>C/<sup>15</sup>N<sub>2</sub> MCU were recorded (not shown). The spectral lines are relatively narrow (FWHH 0.8–2.3 ppm in the <sup>13</sup>C spectrum, 0.5–1.3 ppm in the <sup>15</sup>N spectrum) and well resolved. The <sup>13</sup>C chemical shift (CS) values are  $\delta=54$ , 155, and 159 ppm. Whilst the line at  $\delta=54$  ppm is assigned to the methoxy carbon atom by virtue of its chemical shift, the assignment of the lines at  $\delta=155$  and 159 ppm to the carbamate and urea carbon atoms is not obvious. This assignment was made unambiguously by using the data from the REDOR experiments (see below) with  $\delta(^{13}\text{C,carbamate})=155$  and  $\delta(^{13}\text{C,urea})=159$  ppm. Interestingly, this order is opposite to that of the <sup>13</sup>C chemical shifts of MCU dissolved in dimethyl sulfoxide (DMSO) ( $\delta(^{13}\text{C,carbamate})=154.9$  and  $\delta(^{13}\text{C,urea})=153.5$  ppm).<sup>[2]</sup> Similar differences between the liquid- and solid-state <sup>13</sup>C CPMAS spectra were found in studies of *n*-octylgluconamide.<sup>[9]</sup> These differences can be attributed to 1) differences in the configurations of MCU in DMSO and in the crystal, and 2) different strengths/geometries of the hydrogen bonds between the <sup>13</sup>C=O urea unit and DMSO molecules in solution and the neighboring molecules in the crystal.

The <sup>15</sup>N CPMAS spectra (not shown) reveal two well-separated strong lines with <sup>15</sup>N CS values of  $\delta=43.5$  ppm for <sup>15</sup>N(amide) and  $\delta=81.5$  ppm for <sup>15</sup>N(imide).

**REDOR distance measurements:** The results of the REDOR distance measurements are presented and discussed below. To simplify the notation of the REDOR experiments the observed nucleus is always underlined, for example, AB-REDOR, where A is the observation channel and B is the dephasing channel.

**Effects of homonuclear dipolar coupling:** Prior to performing the REDOR experiments on <sup>13</sup>C(methoxy)<sup>15</sup>N<sub>2</sub> MCU (<sup>13</sup>C/<sup>15</sup>N<sub>2</sub> MCU for short), we numerically studied the possibly disturbing effects of the homonuclear dipolar coupling between the two <sup>15</sup>N nuclei on the REDOR spectra. For this purpose, three-spin REDOR simulations of the I<sub>2</sub>S- (I=<sup>15</sup>N, observed; S=<sup>13</sup>C, dephasing) and IS<sub>2</sub>-spin system (I=<sup>13</sup>C, observed; S=<sup>15</sup>N, dephasing) were performed. They show that the homonuclear dipolar <sup>15</sup>N coupling has a negligible effect on the <sup>13</sup>C/<sup>15</sup>N REDOR/<sup>15</sup>N/<sup>13</sup>C REDOR experiments. Thus, the three-spin system can be evaluated as a purely heteronuclear IS<sub>2</sub>-spin system without homonuclear couplings.

**$^{13}\text{C}^{15}\text{N}$  REDOR on  $^{15}\text{N}(\text{amide})$  MCU:** To facilitate the unambiguous assignment of the  $^{13}\text{C}$  lines, a  $^{13}\text{C}$  (natural abundance)  $^{15}\text{N}$  REDOR spectrum of  $^{15}\text{N}(\text{amide})$ -labeled MCU was recorded. This experiment allows the simultaneous measurement of several  $^{13}\text{C}^{15}\text{N}$  dipolar couplings. From the simulations of the REDOR decay (data not shown), the following dipolar couplings were extracted:  $D = 1100(100)$  Hz, corresponding to a C–N distance of  $1.41(4)$  Å for the line at  $\delta = 159$  ppm,  $D = 125(10)$  Hz, corresponding to  $2.91(8)$  Å for the line at  $\delta = 155$  ppm, and  $D = 80(10)$  Hz, corresponding to  $3.38(14)$  Å for the line of the  $^{13}\text{C}(\text{methoxy})$  atom at  $\delta = 54$  ppm. These data allow the unequivocal assignment of the lines at  $\delta = 159$  and  $155$  ppm to  $^{13}\text{C}(\text{urea})$  and  $^{13}\text{C}(\text{carbamate})$ , respectively, since the strongest dipolar coupling is obviously caused by the direct bond between  $^{15}\text{N}(\text{amide})$  and  $^{13}\text{C}(\text{urea})$ .

Whilst there is no doubt about the intramolecular nature of the dipolar coupling between  $^{15}\text{N}(\text{amide})$  and  $^{13}\text{C}(\text{urea})$ , the question arises as to whether the observed couplings from  $^{15}\text{N}(\text{amide})$  to  $^{13}\text{C}(\text{carbamate})$  and to  $^{13}\text{C}(\text{methoxy})$  are of intramolecular or of intermolecular origin.

- For  $^{13}\text{C}(\text{carbamate})$ , an intermolecular hydrogen bond between  $^{15}\text{N}(\text{amide})$  and  $^{13}\text{C}(\text{carbamate})$  can be excluded as the origin of this dipolar coupling since typical  $\text{CO}\cdots\text{HN}$  hydrogen bonds have distances of typically  $\geq 3.7$  Å. Thus the measured  $2.91(8)$  Å distance is the intramolecular distance between  $^{15}\text{N}(\text{amide})$  and  $^{13}\text{C}(\text{carbamate})$ . Conversion of this three-bond distance into a torsion angle shows that the N(amide)–C(urea)–N(imide)–C(carbamate) part of the molecule adopts a *cis* arrangement since typical C–N distances are  $2.8$  Å for the *cis* arrangement compared with  $3.6$  Å for the *trans* arrangement (Figure 4). In other words, the configuration is *E* at  $\Psi_1$  (see Figure 1).
- For  $^{13}\text{C}(\text{methoxy})$ , an intramolecular C–N distance of  $3.38(14)$  Å is not compatible with any sterically allowed configuration of MCU (see Figure 1), which all have C–N distances  $> 4.0$  Å. Hence, we conclude that this dipolar coupling is of intermolecular origin. This conclusion is corroborated by isotope dilution experiments (see below).

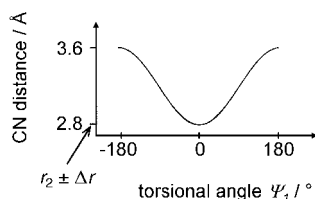


Figure 4. The three-bond C(carbamate)–N(amide) distance as a function of the torsion angle  $\Psi_1$ . Limiting distances for *cis* ( $2.8$  Å) and *trans* ( $3.6$  Å) configurations are from ab initio calculations. The measured distance of  $2.9 \pm 0.1$  Å indicates a *cis* configuration at  $\Psi_1$  for the planar molecule (shaded area).

**$^{15}\text{N}^{13}\text{C}$  REDOR on  $^{13}\text{C}(\text{methoxy})^{15}\text{N}_2$  MCU:** Figure 5 shows the results of the  $^{15}\text{N}^{13}\text{C}$  REDOR experiments of  $^{13}\text{C}^{15}\text{N}_2$  MCU. Both  $^{15}\text{N}(\text{amide})$  and  $^{15}\text{N}(\text{imide})$  exhibit a similar REDOR decay. Simulation of the data employing the model

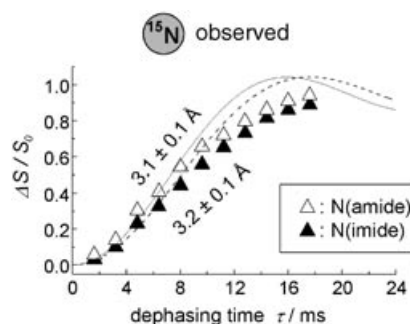


Figure 5.  $^{15}\text{N}^{13}\text{C}$  REDOR data for  $^{13}\text{C}^{15}\text{N}_2$  MCU (undiluted = 100%). Experimental data are shown as triangles, simulations as lines. The solid triangles and the solid line correspond to  $^{15}\text{N}(\text{imide})$ , open triangles and the dashed line correspond to  $^{15}\text{N}(\text{amide})$ . Simulations take the isolated IS spin pair into account and focus on the initial slope of the REDOR decay. Both simulations exhibit pronounced deviations at longer dephasing times, which indicate the presence of at least one additional dipolar coupling.

of a single IS spin pair yields REDOR decay curves that exhibit pronounced deviations from the experimental data at longer dephasing times. This indicates the presence of one or more additional  $^{15}\text{N}^{13}\text{C}$  dipolar coupling(s).

To identify whether the additional coupling is intra- or intermolecular in nature, a dilution experiment was performed (see Figure 6a). The initial slope of this REDOR decay is considerably smaller than that of the undiluted  $^{13}\text{C}^{15}\text{N}_2$  MCU. This shows that the dominant dipolar coupling in neat  $^{13}\text{C}^{15}\text{N}_2$  MCU is of intermolecular origin. Since there is still a 17% chance of intermolecular couplings in the diluted

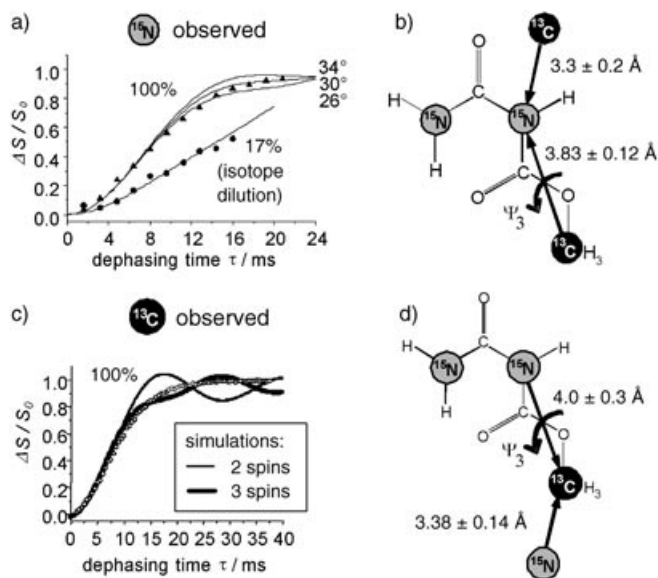


Figure 6. a)  $^{15}\text{N}^{13}\text{C}$  REDOR data for the  $^{15}\text{N}(\text{imide})$  signal of  $^{13}\text{C}^{15}\text{N}_2$  MCU. Data for undiluted  $^{13}\text{C}^{15}\text{N}_2$  MCU (100%) are reproduced from Figure 5. Data for  $^{13}\text{C}^{15}\text{N}_2$  MCU diluted (1:5) in unlabeled MCU show that the dominant coupling has an intramolecular origin. The corresponding simulation takes a combination of IS and  $\text{IS}_2$  spin systems into account. b) A sketch of the molecular structure of  $^{13}\text{C}^{15}\text{N}_2$  MCU indicating intra- and intermolecular C(methoxy)–N(imide) distances. c)  $^{13}\text{C}^{15}\text{N}$  REDOR data for  $^{13}\text{C}^{15}\text{N}_2$  MCU, experimental points and simulations as IS and  $\text{IS}_2$  spin systems. d) A sketch of the molecular structure indicating intra- and intermolecular C(methoxy)–N(imide/amide) distances.

sample, this curve cannot be directly employed in the determination of the intramolecular coupling. Therefore a self-consistent approach was employed. 1) From the simulation of the REDOR curve of the diluted sample employing an IS spin system, a starting value for the intramolecular coupling was determined. 2) This intramolecular coupling was then used in the simulation of the IS<sub>2</sub> spin system of the undiluted sample. From this simulation, the strength of the stronger coupling and the angle between the two distance vectors were determined. 3) These values were employed in an improved simulation of the diluted curve in which the IS and IS<sub>2</sub> spin systems were statistically superimposed. Steps 2 and 3 were repeated until a self-consistent set of dipolar couplings and angles was determined. The resulting dipolar couplings and the corresponding distances and angles between the two distance vectors are collected in Table 1. The intra- and intermolecular distances for N(imide) are shown in Figure 6b. Similar results are obtained for N(amide).

Table 1. Values of the parameters  $D_1$ ,  $D_2$ , and  $\theta$  extracted from the simulations of the  $^{13}\text{C}^{15}\text{N}$  REDOR data for  $^{13}\text{C}(\text{methoxy})^{15}\text{N}_2$  MCU. From the dilution experiments it is evident that  $D_1$  is the intermolecular and  $D_2$  the intramolecular coupling.

N	$D_1$ [Hz]	$D_2$ [Hz]	$\theta$ [°]
imide	90(15)	55(5)	30(5)
	3.3(2) Å	3.83(12) Å	30(5)
amide	90(15)	34(4)	30(5)
	3.3(2) Å	4.5(2) Å	30(5)

**$^{13}\text{C}^{15}\text{N}$  REDOR on  $^{13}\text{C}(\text{methoxy})^{15}\text{N}_2$  MCU:** In order to complete the REDOR experiments for the  $^{13}\text{C}(\text{methoxy})^{15}\text{N}_2$  MCU sample, “inverse”  $^{13}\text{C}^{15}\text{N}$  REDOR experiments were performed in which the observation and dephasing channels were exchanged (“inverse”) with respect to the experiments described in the previous Section. Figure 6c displays the experimental REDOR decay of  $^{13}\text{C}(\text{methoxy})$ , which shows a monotonic growth of the dephasing with no pronounced features, which would be expected for IS and IS<sub>2</sub> spin systems (simulations inside figure). This featureless shape of the decay curve can be understood if one takes into account that in addition to the couplings shown in Figure 6d, there are at least two additional couplings to other amide and imide nitrogen atoms, which are expected from the results of experiments described above. These additional couplings result in an IS<sub>4</sub> or higher spin system, which leads to an experimental REDOR decay curve that cannot be evaluated quantitatively, even if some of the couplings are already known. Accordingly only the structural constraints from the  $^{15}\text{N}^{13}\text{C}$  REDOR experiments have been used in the discussion on the results from REDOR experiments.

**$^{13}\text{C}^{15}\text{N}$  REDOR on a 1:1 mixture of  $^{13}\text{C}(\text{urea})$  and  $^{15}\text{N}(\text{amide})$  MCU:** Intermolecular couplings can be exploited to gain information about the molecular packing of the MCU molecules in a crystal. In the present case, possible packing patterns involve the hydrogen acceptor and donor groups,  $\text{NH}_2(\text{amide})$  and  $\text{C}=\text{O}(\text{urea})$ , in amides,<sup>[44,45]</sup> methyl carbamate,<sup>[46]</sup> and in urea/biuret derivatives, for example,

$\text{N},\text{N}'$ -diacetylbiuret<sup>[47]</sup> and  $\text{MCB}\cdot\text{H}_2\text{O}$ .<sup>[1]</sup> The question, does an intramolecular  $\text{C}=\text{O}\cdots\text{H}-\text{N}$  bond exist between these groups in MCU?, can be answered with the results of a REDOR experiment on a cocrystallized 1:1 mixture of  $^{13}\text{C}(\text{urea})$  MCU and  $^{15}\text{N}(\text{amide})$  MCU. If this hydrogen bond exists, 50% of the  $^{13}\text{C}$  atoms will be exposed to  $^{13}\text{C}^{15}\text{N}$  heteronuclear coupling and the other 50% of  $^{13}\text{C}$  atoms will be exposed to  $^{13}\text{C}^{13}\text{C}$  homonuclear coupling, which has no or only a negligible effect on the REDOR spectra. The corresponding explanation holds for the  $^{15}\text{N}$  spins.

Because of the higher sensitivity of  $^{13}\text{C}$  compared to  $^{15}\text{N}$  in SSNMR, a  $^{13}\text{C}^{15}\text{N}$  REDOR experiment was performed on a nominally 1:1 cocrystallized mixture of  $^{13}\text{C}(\text{urea})$  MCU and  $^{15}\text{N}(\text{amide})$  MCU (Figure 7). The exact composition of

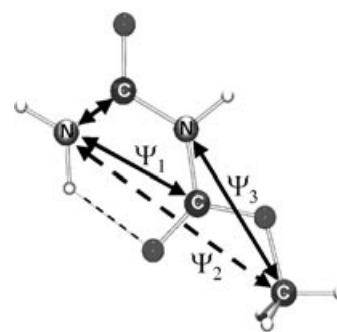


Figure 7.  $^{13}\text{C}^{15}\text{N}$  REDOR data and simulation curves for  $^{13}\text{C}(\text{urea})$  in a 1:1 mixture of  $^{13}\text{C}(\text{urea})$  MCU and  $^{15}\text{N}(\text{amide})$  MCU. Solid lines: simulations on the basis of isolated IS spin pairs yielding  $D=80(10)$  Hz, which corresponds to 3.5(2) Å.

the 1:1 mixture of  $^{13}\text{C}(\text{urea})$  MCU and  $^{15}\text{N}(\text{amide})$  MCU was determined from a liquid-state  $^1\text{H}$  NMR spectrum of the dissolved cocrystallized sample, which revealed a composition of 51.6%  $^{13}\text{C}$  MCU and 48.4%  $^{15}\text{N}$  MCU. From these data, the expected REDOR decay at long dephasing times is  $\Delta S/S_0=0.48$ . The REDOR curve was evaluated by employing this value. An intermolecular dipolar coupling of  $D=80(10)$  Hz, corresponding to a C–N distance of 3.5(2) Å (see Figure 7), was obtained.

**Discussion of the results of REDOR experiments:** The distance and angle data are collected in Table 1 and Table 2. Intramolecular distances are presented in Figure 8. In the following discussion, they are interpreted and combined to yield the structure of MCU. This interpretation was achieved in two steps: first the molecular conformation of MCU was determined by employing the intramolecular distance constraints and then the molecular packing of MCU was investigated by employing the intermolecular distance constraints.

Table 2. Values of the parameters  $D_1$ ,  $D_2$ , and  $\theta$  extracted from the simulations of the  $^{13}\text{C}^{15}\text{N}$  REDOR data for  $^{13}\text{C}^{15}\text{N}_2$  MCU.

$D_1$ [Hz]	$D_2$ [Hz]	$\theta$ [°]
80(10)	50(10)	25(10)
3.4(2) Å	4.0(3) Å	25(10)

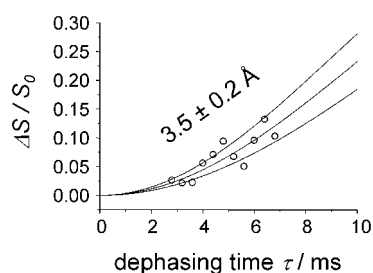


Figure 8. *EEZ* configuration of MCU, determined from an ab initio calculation using the distance constraints from the REDOR experiments. The REDOR distance constraints are shown as double arrows; the dashed arrow indicates the long C–N distance, which is determined as  $\geq 4.5(2)$  Å. An intramolecular hydrogen bond is formed between the N(amide) and the O(carbamate) atoms.

**Molecular configuration of MCU:** The three torsion angles  $\Psi_1$ ,  $\Psi_2$  and  $\Psi_3$  determine the configuration of MCU.  $\Psi_1$  and  $\Psi_3$  can be obtained from the conversion of the corresponding three-bond distances. Namely, the intramolecular  $^{15}\text{N}(\text{amide})\text{--}^{13}\text{C}(\text{carbamate})$  distance yields  $\Psi_1$ , which is about  $0^\circ$ , that is, the configuration is *E* at  $\Psi_1$  (see Figure 1). The intramolecular dipolar coupling for N(imide) to C(methoxy),  $D_2 = 55(5)$  Hz, allows the determination of the configuration at  $\Psi_3$  (see Figure 6b). The dipolar couplings expected for the *cis* and *trans* arrangements of the N(imide)–C(carbamate)–O(methoxy)–C(methoxy) unit are 150 (2.7 Å) and 60 Hz (3.7 Å), respectively. Clearly, the *trans* configuration, which in this case corresponds to the *Z* configuration, is found for  $\Psi_3$  of MCU (see Figure 6b).

The torsion angle  $\Psi_2$  can be determined indirectly from the five-bond distance between N(amide) and C(methoxy),  $D_2 = 34(4)$  Hz. This coupling is not compatible with the *EZZ* configuration of MCU, which would have a stronger dipolar coupling of approximately 50 Hz (see Figure 1).

By combining these constraints, it is evident that MCU adopts the *EEZ* configuration. The gas-phase calculations also showed this configuration to be more stable than the *EZZ* (+4.3 kcal mol $^{-1}$ ), *EEE* (+10.1 kcal mol $^{-1}$ ) and *ZEZ* (+10.2 kcal mol $^{-1}$ ) configurations. Here the low energies of the *EEZ* and *EZZ* configurations are a result of the intramolecular hydrogen bond between N(amide) and C=O(carbamate). Thus one can conclude that the formation of this intramolecular hydrogen bond is a major factor stabilizing the configuration of MCU.

**Intermolecular arrangement of MCU:** Before creating a structural model of MCU, the salient results have been collected. 1) From the calculations and REDOR experiments described above it is evident that the MCU molecule is planar.

From the 1:1 mixture of  $^{13}\text{C}(\text{urea})$  MCU and  $^{15}\text{N}(\text{amide})$  MCU, the following additional structural information about the intermolecular arrangement of MCU has been obtained. 2) The observed intermolecular C–N distance of  $3.5(2)$  Å is in good agreement with typical C–N distances found in linear  $\text{C}=\text{O}\cdots\text{H}\text{--}\text{N}$  hydrogen bonds, in which an O–N distance of 2.9 Å corresponds to a C–N distance of 3.7 Å. 3) From the REDOR experiments performed on  $^{13}\text{C}^{15}\text{N}_2$  MCU,

an intermolecular C–N distance of  $3.4(2)$  Å was found both between C(methoxy) and N(imide) and between C(methoxy) and N(amide). No hydrogen bonding or other direct interaction between the carbon and nitrogen atoms of two neighboring molecules is expected. 4) From simulations of the  $\text{IS}_2$  spin system an angle  $\chi(^{13}\text{C}^{15}\text{N}^{13}\text{C})$  of  $30^\circ$  or  $180\text{--}30^\circ$  was obtained for both the amide and imide nitrogen.

Owing to 1) it is not possible to create MCU oligomers in which all the hydrogen bond donors and acceptors are saturated. This result is corroborated by ab initio calculations, which reveal that MCU molecules are more likely to form planar strip-like chains. Inside these chains the hydrogen bond donors and acceptors are saturated and the methoxy groups form the borders of the chains.

By employing a molecular modeling program we were able to find three different possible molecular arrangements of the MCU in these chains (Figure 9). All three motifs are characterized by an intermolecular hydrogen bond between C(urea) and N(amide) following from distance constraint 2). In the first two cases (**I**, **II**) there are two hydrogen bonds between C(urea) and N(amide) and two hydrogen bonds between C(urea) and N(imide), forming two-fold dimers either of  $\text{C}_2$  symmetry (**I**) or of mirror glide symmetry (**II**). Motif **III** is a chain with  $\text{C}_2$  glide symmetry formed by hydrogen bonds between C(urea) and N(amide). Ab initio calculations on these motifs showed that arrangements **I** and **II** are energetically favored over arrangement **III**, which is a consequence of the higher number of stabilizing hydrogen bonds and more compact packing in motifs **I** and **II**.

All three motifs have chains of linked MCU molecules with methoxy groups at the borders. These chains interact through these methoxy groups to form layers that consist of parallel or antiparallel chains. For these models the short intermolecular C(methoxy)–N(amide or imide) distances of  $3.3(2)$  and  $3.4(2)$  Å, respectively, and the CNC angles of about  $30^\circ$  cannot both be realized in a single layer since the nitrogen atoms are located in the interior of each chain (Figure 9). Thus one can conclude that these short intermolecular distances are between different layers. This conclusion is corroborated by the fact that the measured distances are comparable to typical interlayer distances of other (planar) organic substances, which are of the order of  $3.2$  Å $^{[48]}$  for example, cyanuric acid and melamine. $^{[49]}$  From the data presented here it is not possible to determine whether these layers are parallel or skewed.

## Conclusion

The study presented here shows the structure determination of organic compounds by dipolar solid-state NMR spectroscopy. Our strategy was based on the application of precise REDOR measurements of strategic intra- and intermolecular C–N distances. Isotope dilution experiments and numerical simulations of  $\text{IS}_n$  spin systems were used to discriminate between intra- and intermolecular dipolar couplings and to quantify them. By employing the dipolar couplings, first the molecular configuration of the molecule was determined and then the packing of the molecules was analyzed.



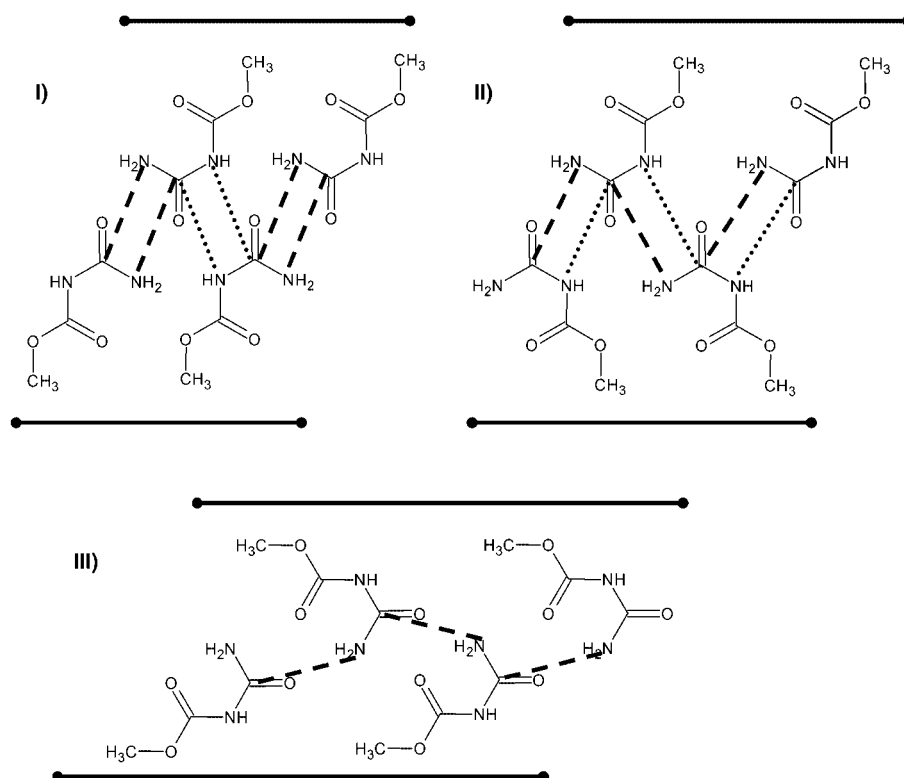


Figure 9. Possible arrangements of MCU molecules in a layer. Chains of hydrogen-bonded molecules are continued to the left and right sides; the upper and lower sides are bordered by methoxy groups (see horizontal lines). C=O(urea)⋯H–N hydrogen bonds are indicated a) by dashed lines from C(urea) to N(amide) and b) by dotted lines from C(urea) to N(imide). Intramolecular hydrogen bonds and NH(amide)⋯OCH<sub>3</sub> hydrogen bonds are omitted for clarity. **I**: twofold dimers ( $C_2$  symmetry), **II**: twofold dimers (mirror glide symmetry), **III**: chain ( $C_2$  glide symmetry).

The determination of the molecular configuration of MCU was performed in three steps: 1) distance constraints of structural subunits of the molecule were determined from REDOR experiments on selectively labeled isotopomers, 2) torsion angles in these subunits were calculated from the distance constraints, and 3) the resulting configurations were compared with all possible configurations of MCU, which were determined by ab initio calculations.

The configuration of the MCU molecule was determined by three torsion angles  $\Psi_1$ ,  $\Psi_2$ , and  $\Psi_3$ . Ab initio calculations show that all these angles are either 0° or 180° (*Z* or *E*). From the REDOR experiments, the *E* configuration was found for  $\Psi_1$  and  $\Psi_2$  and the *Z* configuration for  $\Psi_3$ . Thus the configuration of MCU in the solid state was determined to be *EEZ*.

Distance constraints for the intermolecular arrangement of MCU were obtained from REDOR experiments on  $^{13}\text{C}^{15}\text{N}_2$  MCU with different degrees of isotope dilution and on a cocrystallized 1:1 mixture of  $^{13}\text{C}$ (urea) MCU and  $^{15}\text{N}$ (amide) MCU. By combining these distance constraints with molecular modeling, three different possible packing motifs for MCU molecules were identified. All these motifs have molecules that are arranged as linear chains with the methoxy groups at the borders of the chain and intermolecular hydrogen bond donors and acceptors that are all saturated in the interior of the chain.

The results presented in this article may be extended by performing homonuclear  $^{13}\text{C}$ – $^{13}\text{C}$  correlation experiments

and more detailed calculations on the molecular packing. These may be helpful to decide between possible stacking patterns using the structural constraints obtained in this study and may lead to true “NMR crystallography” in the future.

## Acknowledgements

This work was supported by the Deutsche Forschungsgemeinschaft, DFG, SFB-498. S.M. gratefully acknowledges a postdoctoral grant from the DFG Graduiertenkolleg GK-788. The authors thank Prof. H.-H. Limbach for helpful discussions.

- [1] F. Börner, *Synthese, Charakterisierung und Untersuchung von schwerlöslichen Harnstoffderivaten als Grundlage für Düngemittel*, PhD Thesis, FU Berlin, **2000**.
- [2] S. Macholl, F. Börner, G. Buntkowsky, *Z. Phys. Chem. (Muenchen Ger.)* **2003**, 217, 1473–1505.
- [3] G. Buntkowsky, I. Sack, H.-H. Limbach, B. Kling, J. Fuhrhop, *J. Phys. Chem. B* **1997**, 101, 11 265–11 272.
- [4] F. Taulelle, C. Gérardin, M. Haouas, C. Huguenard, V. Munch, T. Loiseau, G. Férey, *J. Fluorine Chem.* **2000**, 101, 269–272.
- [5] S. M. Reutzel-Edens, V. A. Russell, L. Yu, *J. Chem. Soc., Perkin Trans. 2* **2000**, 913–924.
- [6] F. Taulelle, C. Huguenard, *Stud. Surf. Sci. Catal.* **2001**, 135.
- [7] S. M. Reutzel-Edens, J. K. Bush, *Am. Pharm. Rev.* **2002**, 5, 112–115.
- [8] K. Schmidt-Rohr, *J. Am. Chem. Soc.* **1996**, 118, 7601.
- [9] S. Macholl, I. Sack, H.-H. Limbach, J. Pauli, M. Kelly, G. Buntkowsky, *Magn. Reson. Chem.* **2000**, 38, 596.

- [10] I. Sack, Y. S. Balazs, S. Rahimpour, S. Vega, *J. Magn. Reson.* **2001**, *148*, 104–114.
- [11] E. Hughes, J. Jordan, T. Gullion, *J. Phys. Chem. B* **2001**, *105*, 5887–5891.
- [12] E. Hughes, T. Gullion, A. Goldbourt, S. Vega, A. J. Vega, *J. Magn. Reson.* **2002**, *156*, 230–241.
- [13] G. Goobes, S. Vega, *J. Magn. Reson.* **2002**, *154*, 236–251.
- [14] A. Goldbourt, S. Vega, T. Gullion, A. J. Vega, *J. Am. Chem. Soc.* **2003**, *125*, 11194–11195.
- [15] T. Gullion, R. Kishore, T. Asakura, *J. Am. Chem. Soc.* **2003**, *125*, 7510–7511.
- [16] T. Gullion, J. Schaefer, *Adv. Magn. Opt. Reson.* **1989**, *13*, 57.
- [17] SPARTAN, Wavefunction, Inc., 18401 Karman Avenue, Suite 370, Irvine, CA 92612 (USA), **1995**.
- [18] K. T. Mueller, T. P. Jarvie, D. J. Aurentz, B. W. Roberts, *Chem. Phys. Lett.* **1995**, *242*, 535.
- [19] J. D'espinoze De La Caillerie, C. Fretigny, *J. Magn. Reson.* **1998**, *133*, 273.
- [20] J. M. Goetz, J. Schaefer, *J. Magn. Reson.* **1997**, *127*, 147.
- [21] C. A. Fyfe, A. R. Lewis, J. M. Chezeau, H. Grondey, *J. Am. Chem. Soc.* **1997**, *119*, 12210–12222.
- [22] M. Bertmer, H. Eckert, *Solid State Nucl. Magn. Reson.* **1999**, *15*, 139–152.
- [23] C. A. Michal, L. W. Jelinski, *J. Am. Chem. Soc.* **1997**, *119*, 9059–9060.
- [24] A. E. Bennett, L. R. Becerra, R. G. Griffin, *J. Chem. Phys.* **1994**, *100*, 812.
- [25] A. E. Bennett, C. M. Rienstra, P. T. Lansbury, R. G. Griffin, *J. Chem. Phys.* **1996**, *105*, 10289.
- [26] T. Gullion, C. Pennington, *Chem. Phys. Lett.* **1998**, *290*, 88–93.
- [27] O. Liivak, D. B. Zax, *J. Chem. Phys.* **2000**, *113*, 1088–1096.
- [28] Gaussian 98, Rev. B. 2, M. J. Frisch, G. W. Trucks, H. B. Schlegel, G. E. Scuseria, M. A. Robb, J. R. Cheeseman, V. G. Zakrzewski, J. Montgomery, Jr., R. E. Stratman, J. C. Burant, S. Dapprich, J. M. Millam, A. D. Daniels, K. N. Kudin, M. C. Strain, O. Farkas, J. Tomasi, V. Barone, M. Cossi, R. Cammi, B. Mennucci, C. Pomelli, C. Adamo, S. Clifford, J. Ochterski, G. A. Petersson, P. Y. Ayala, Q. Cui, K. Morokuma, D. K. Malick, A. D. Rabuck, K. Raghavachari, J. B. Foresman, J. Cioslowski, J. V. Ortiz, A. G. Baboul, B. B. Stefanov, G. Liu, A. Liashenko, P. Piskorz, I. Komaromi, R. Gomperts, R. L. Martin, D. J. Fox, T. Keith, M. A. Al-Laham, C. Y. Peng, A. Nanayakkara, C. Gonzalez, M. Challacombe, P. M. W. Gill, B. Johnson, W. Chen, M. W. Wong, J. L. Andres, C. Gonzales, M. Head-Gordon, E. S. Replogle, J. A. Pople, Gaussian, Inc., Pittsburgh, PA, **1998**.
- [29] A. D. Becke, *J. Chem. Phys.* **1993**, *98*, 5648.
- [30] C. Lee, W. Yang, R. G. Parr, *Phys. Rev. B* **1988**, *37*, 785.
- [31] A. E. Bennett, C. M. Rienstra, M. Auger, K. V. Lakshmi, R. G. Griffin, *J. Chem. Phys.* **1995**, *103*, 6951.
- [32] G. Metz, X. Wu, S. O. Smith, *J. Magn. Reson., Ser. A* **1994**, *110*, 219–227.
- [33] T. Gullion, D. B. Baker, M. S. Conradi, *J. Magn. Reson.* **1990**, *89*, 479.
- [34] T. Gullion, J. Schaefer, *J. Magn. Reson.* **1991**, *92*, 439.
- [35] Y. Li, J. N. S. Evans, *J. Magn. Reson., Ser. A* **1995**, *116*, 150.
- [36] T. Gullion, J. Schaefer, *J. Magn. Reson.* **1989**, *81*, 196.
- [37] A. E. Bennett, R. G. Griffin, S. Vega, *Springer Series in NMR* **1994**, *33*.
- [38] J. Garbow, T. Gullion in *Carbon-13 NMR Spectroscopy of Biological Systems* (Ed.: N. Beckmann), Academic Press Inc., New York, **1995**, pp. 65–115.
- [39] I. Sack, S. Macholl, J. H. Fuhrhop, G. Buntkowsky, *Phys. Chem. Chem. Phys.* **2000**, *2*, 1781.
- [40] A. Naito, K. Nishimura, S. Tuzi, H. Saito, *Chem. Phys. Lett.* **1994**, *229*, 506–511.
- [41] K. Nishimura, A. Naito, S. Tuzi, H. Saito, *J. Phys. Chem. B* **1999**, *103*, 8398–8404.
- [42] M. Bak, J. T. Rasmussen, N. C. Nielsen, *J. Magn. Reson.* **2000**, *147*, 296–330.
- [43] M. Bak, N. C. Nielsen, *J. Magn. Reson.* **1997**, *125*, 132–139.
- [44] L. Leiserowitz, M. Tuval, *Acta Crystallogr. Sect. B* **1978**, *34*, 1230–1247.
- [45] J. C. Williams, A. E. McDermott, *J. Phys. Chem. B* **1998**, *102*, 6248–6259.
- [46] B. Sepehrnia, J. R. Ruble, G. A. Jeffrey, *Acta Crystallogr. Sect. C* **1987**, *43*, 249–251.
- [47] S. Macholl, *Determination of Molecular Structures by Dipolar Solid State NMR Spectroscopy*, PhD Thesis, FU Berlin, **2002**.
- [48] A. I. Kitaigorodski, *Molekülkristalle*, 1st ed., Akademie-Verlag, Berlin, **1979**.
- [49] Y. Wang, B. Wei, Q. Wang, *J. Crystallogr. Spectrosc. Res.* **1990**, *20*, 1990.

Received: February 27, 2004  
Published online: August 17, 2004